Atmospheric Wake Phenomena near the Canary Islands

LEON I. ZIMMERMAN[1]

University of Oklahoma, Norman

(Manuscript received 13 November 1968, in revised form 7 August 1969)

ABSTRACT

The von Kármán theory of vortex trails and the concept of vorticity diffusion are applied to atmospheric vortex trails generated by Tenerife, Gran Canaria and Fuerteventura Islands of the Canary Island group, and a pair of vortices from Madeira Island. This is done in order to calculate effective eddy viscosities, ages, radii, maximum tangential velocities, and kinetic energy dissipation rates of the vortices. As an example, the effective eddy viscosity for the Madeira Island vortex pair is 2×10^7 cm^2 sec^{-1}. One of the vortex pair has an age of 12×10^4 sec (34 hr), a vortex maximum tangential velocity of 3 m sec^{-1} occurring at a radius of 36 km, and its rate of kinetic energy dissipation is 0.2 erg gm^{-1} sec^{-1}. Observed vortex growth rates appear to agree with theory. The results of the study are consistent with previous studies and hypotheses relating to atmospheric mesoscale eddy patterns.

1. Introduction

On 16 December, the Gemini 6 spacecraft crew photographed cloud formations over various regions of the earth. Several photographs of cloud formations were taken in the vicinity of the Canary Islands. Contained in these photographs are vortex trails whose properties appear to be consistent with theories that have evolved in relation to the classical von Kármán vortex street.

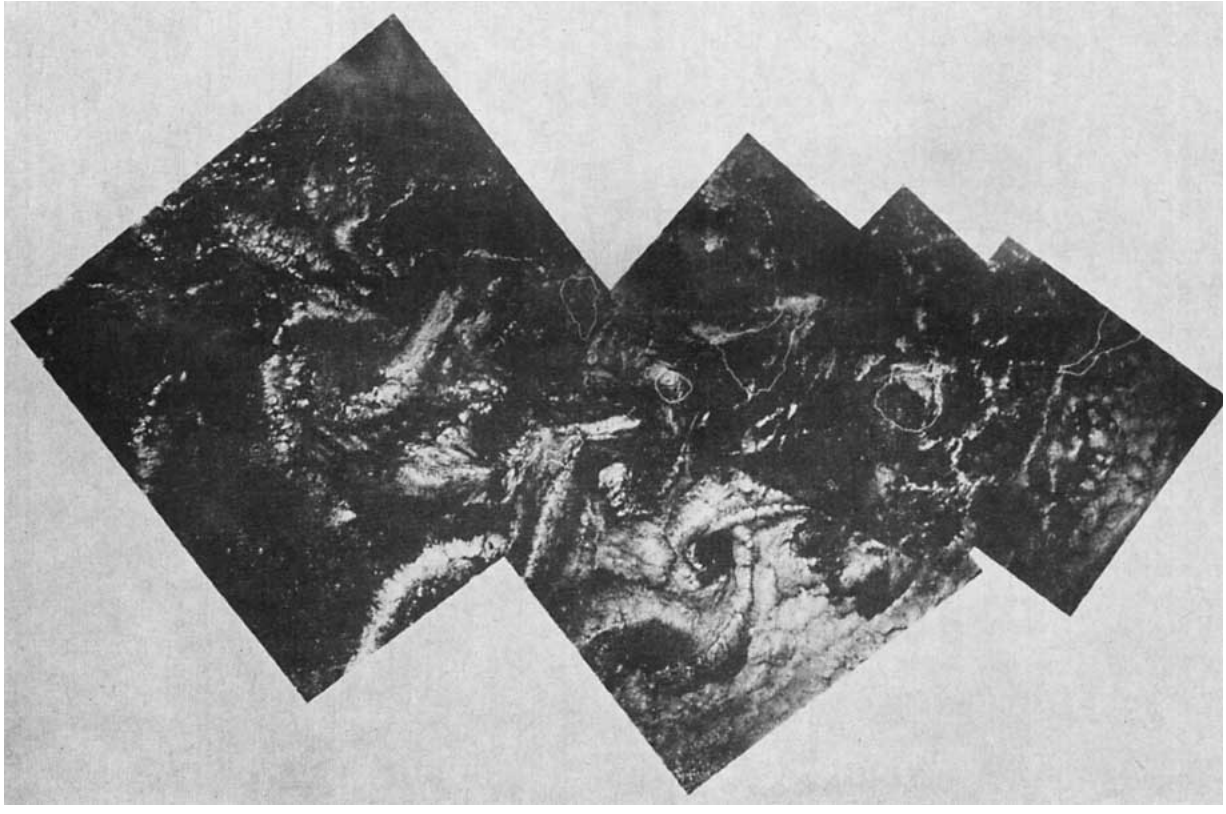

FIG. 1. Mosaic of Gemini 6 photographs of the Canary Island region, 1044 GMT 16 December 1965.

[1] 1st Lieutenant, USAF, now assigned to the Development Section, U. S. Air Force, Environmental Technical Applications Center, Washington, D. C.

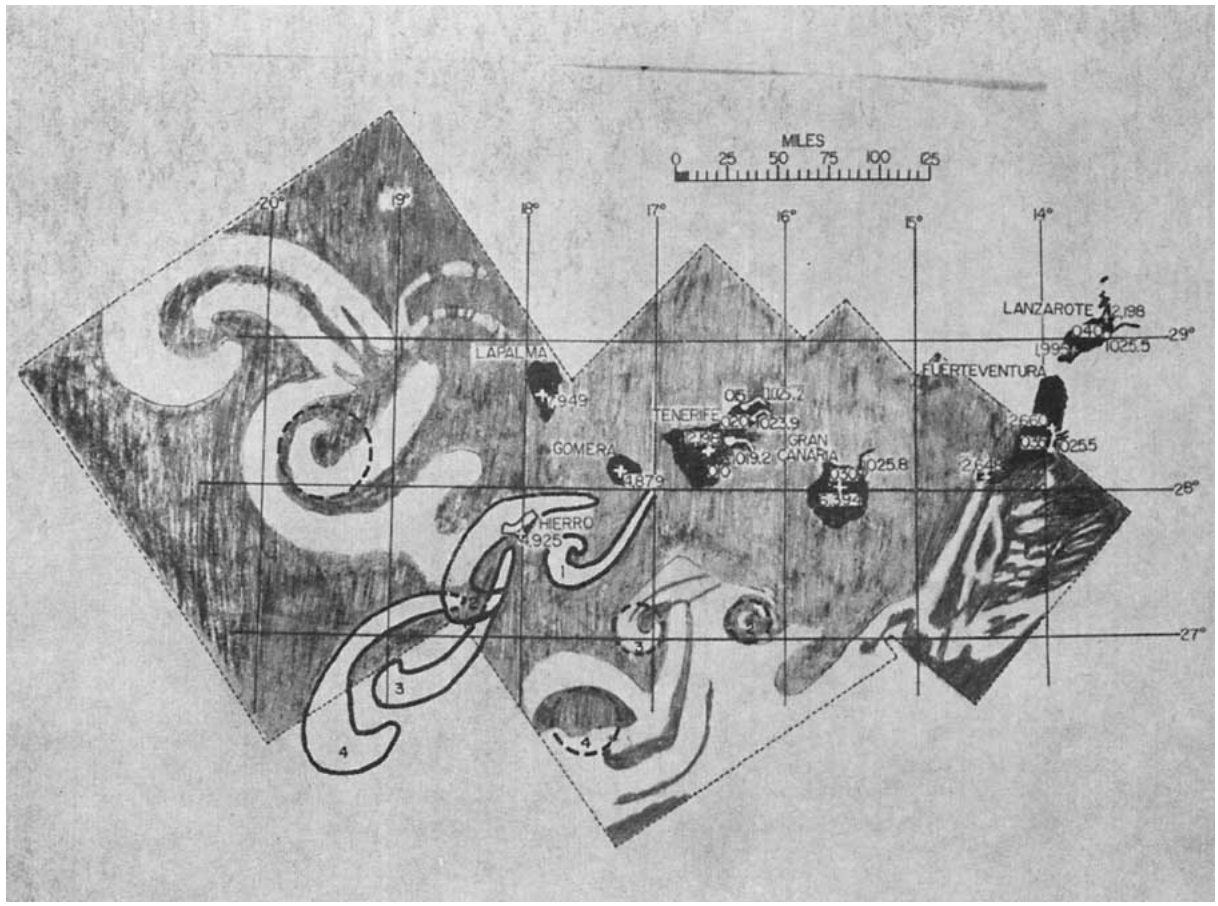

FIG. 2. Artist's concept of the photomosaic, same scale as Fig. 1.

Previous studies of similar trails have been made by Hubert and Krueger (1962) and Chopra and Hubert (1964, 1965).[2] There have been sightings of these trails in the vicinity of other islands and island groups.

Friday and Wilkins (1967) described and illustrated vortex trail phenomena in the lee of the island and island group of Guadalupe and Cape Verde, respectively. This same study cited one trail in the Southern Hemisphere caused by the islands of Mauritius and La Reunion just east of the Malagasy Republic off the eastern coast of Africa. Conover (1964) illustrated and discussed "circular spiral patterns," hereafter referred to as Kármán vortex streets, generated by the Canary and Cape Verde Island groups.

2. Description of the photographs

Because of the nearly vertical orientation of the cameras on Gemini 6, rectification of these photographs is less difficult than for most satellite photographs. A mosaic, assembled from these photographs, shows clouds in the form of vortex trails. The orientation of the trails provides a means of estimating the flow direction for several hours prior to the time of the photographs. This is discussed in relation to a pair of eddies apparently generated from Madeira Island.

Fig. 1 shows the mosaic of photographs taken over the Canary Islands by the Gemini 6 spacecraft at 1044 GMT on 16 December 1965. Fig. 2 is taken from a map of the islands drawn to the same scale as the photomosaic, where the more significant features of the cloud pattern have been sketched for emphasis. The figure shows an area some 500 mi in longitude and approximately 250 mi in latitude. Several different wake trails from the various members of the island group may be seen in the picture. The vortex trail extending southwestward from the island of Tenerife (28.5N, 16.5W) has been extended to show how it might appear in a more extensive picture.

In addition to vortex trails from the Canary Island group, the photomosaic reveals in the left-hand portion a pair of eddies apparently generated from Madeira Island; these may be compared with a similar pair of

[2] Since this paper was written, the author's attention has been drawn to similar literature relevant to the topic presented by Chopra [*Bull. Amer. Phys. Soc. Ser. II*, 11, p. 708 (1966); *Trans. Amer. Geophys. Union*, 49, p. 180 (1968)].

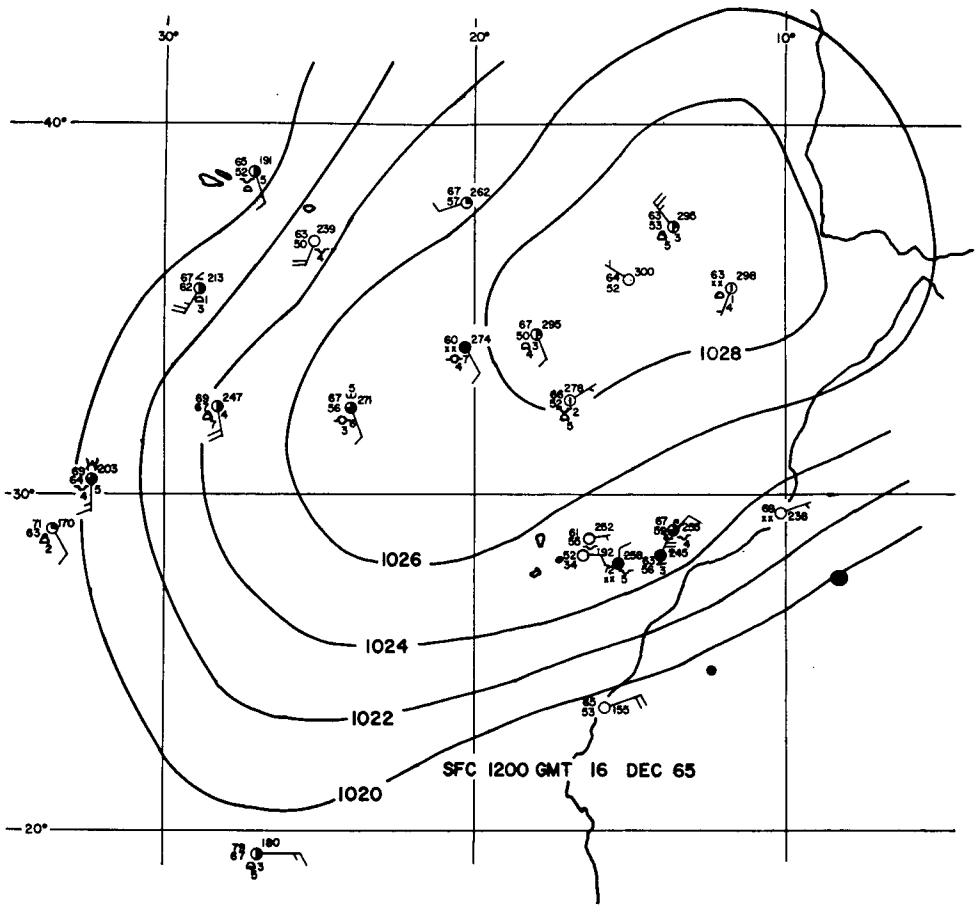

FIG. 3. Author's analysis of suface pressure pattern of Canary Island region for 1200 GMT 16 December 1965.

eddies from Madeira discussed by Chopra and Hubert (1964). The eddies are visible in the stratocumulus clouds. Table 1 gives the positions of Madeira Island and the islands of the Canary group. The various weather stations and altitudes of peaks located on these islands are also noted.

The straight cloud street in Fig. 1 extending southwestward from the 0.8-km peak on Fuerteventura (28.3N, 13.5W) is characteristic of a small Reynolds number ($\lesssim 35$). A small Reynolds number is expected because the diameter of this peak is small compared to the diameters of peaks on the other islands. Wakes similar to the one extending from Fuerteventura have been detected in other satellite cloud photographs.

TABLE 1. Geographical data for Madeira Island and the islands of the Canary Group.

Island	Station	Latitude (N)	Longitude (W)	Peak elevation (km)
La Palma		29	17.9	2.42
Gomera		28.2	17.2	1.49
Tenerife	010 015 020	28.5	16.5	3.72
Gran Canaria	030	28	15.5	1.95
Hierro		27.8	18	1.50
Fuerteventura		N/A	N/A	0.81
Madeira	521	32.75	17	1.86

3. Synoptic discussion

Analysis of synoptic reports (roughly an hour after the photographs were made) confirms an overcast of Type 8 (stratocumulus and cumulus) clouds over Tenerife. The cloud bases are 0.6–1 km above the surface, which places them below the temperature inversion.

The radiosonde report at Santa Cruz de Tenerife prior to the time of the photographs (0000 GMT) showed a fairly strong temperature inversion from 830 to 801 mb, or approximately 1.6–2 km in altitude. The temperature increase is about 3C through the layer, thus giving a temperature gradient of $+7.5$C km^{-1}. The relative humidity is 100% at the inversion base, indicating that the cloud tops extended to at least 1.6 km.

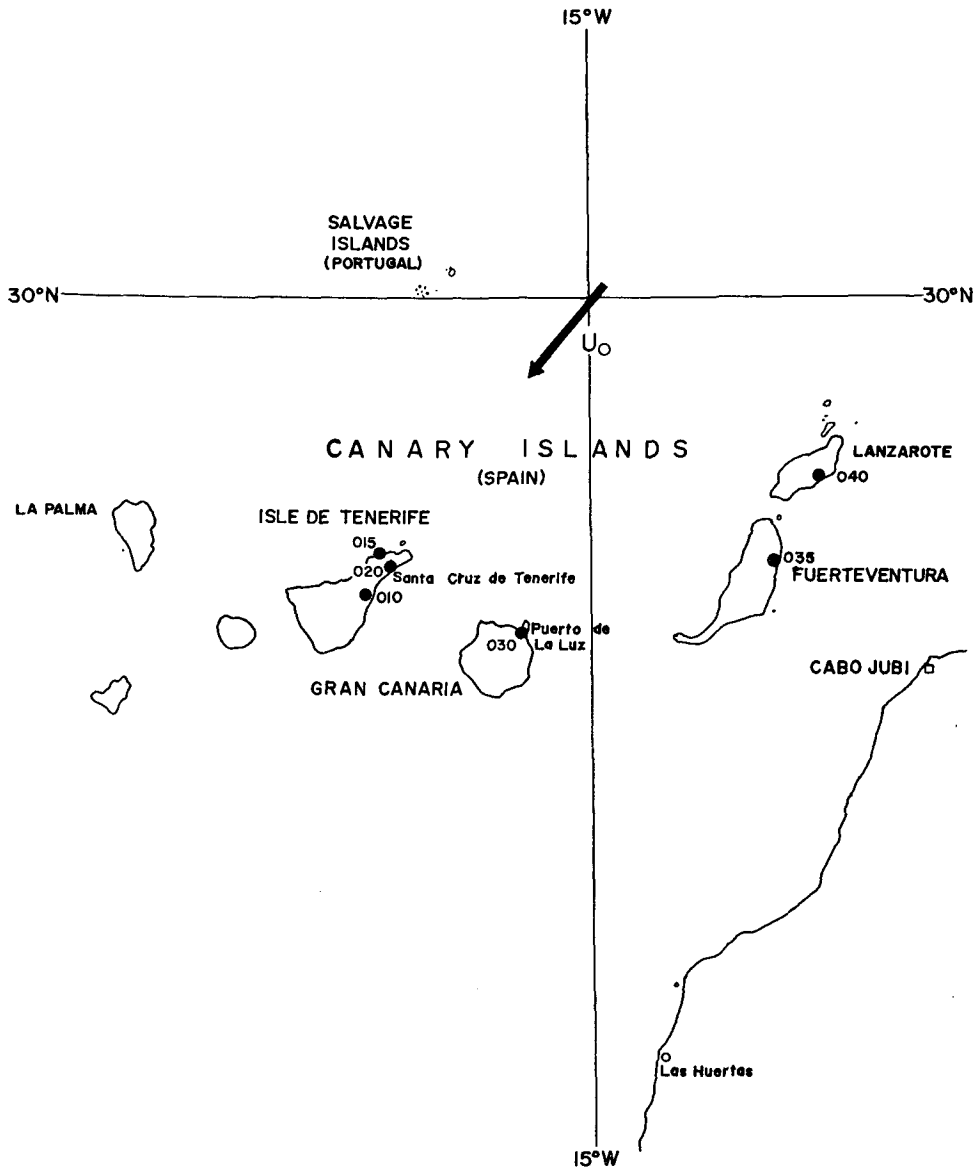

FIG. 4. Orientation of the Canary Island group with respect to the mean wind.

One can be reasonably sure that this subsidence inversion persisted throughout the 12-hr period from 0000–1200 GMT. This is because of the permanence in the location of the subtropical (Azores) anticyclone, with respect to the islands, during that time. Fig. 3 is an analysis, made by the author, of the synoptic pattern for 1200 GMT 16 December 1965. The analysis is based on the photographs and some additional synoptic reports from various land stations and from ships at sea.

Friday and Wilkins (1967) suggest that vortex trail formation is seen only with islands which lie on the eastern side of the subtropical anticyclones. In the present case, the high pressure center is located to the west and north of the island group. The island group is in the lower portion of the high pressure area, or in the area where the maximum lateral spreading of air should be expected. Thus, a subsidence inversion should persist throughout this region.

4. Aerodynamic pressure effects

Wilkins (1968) suggested that a periodic fluctuation in pressure should exist on the steep sides of the islands exposed tangentially to the free stream velocity vector and that these pressure fluctuations, caused by flow separation during vortex shedding, might have a magnitude possibly as great as 1 mb.

The location of the six stations of the Canary Island group is shown in Fig. 4. Stations 010, 035 and 040 are located on the sides of the islands and are thus exposed to the free-stream velocity (represented by $\mathbf{U}_0$ in Fig. 4),

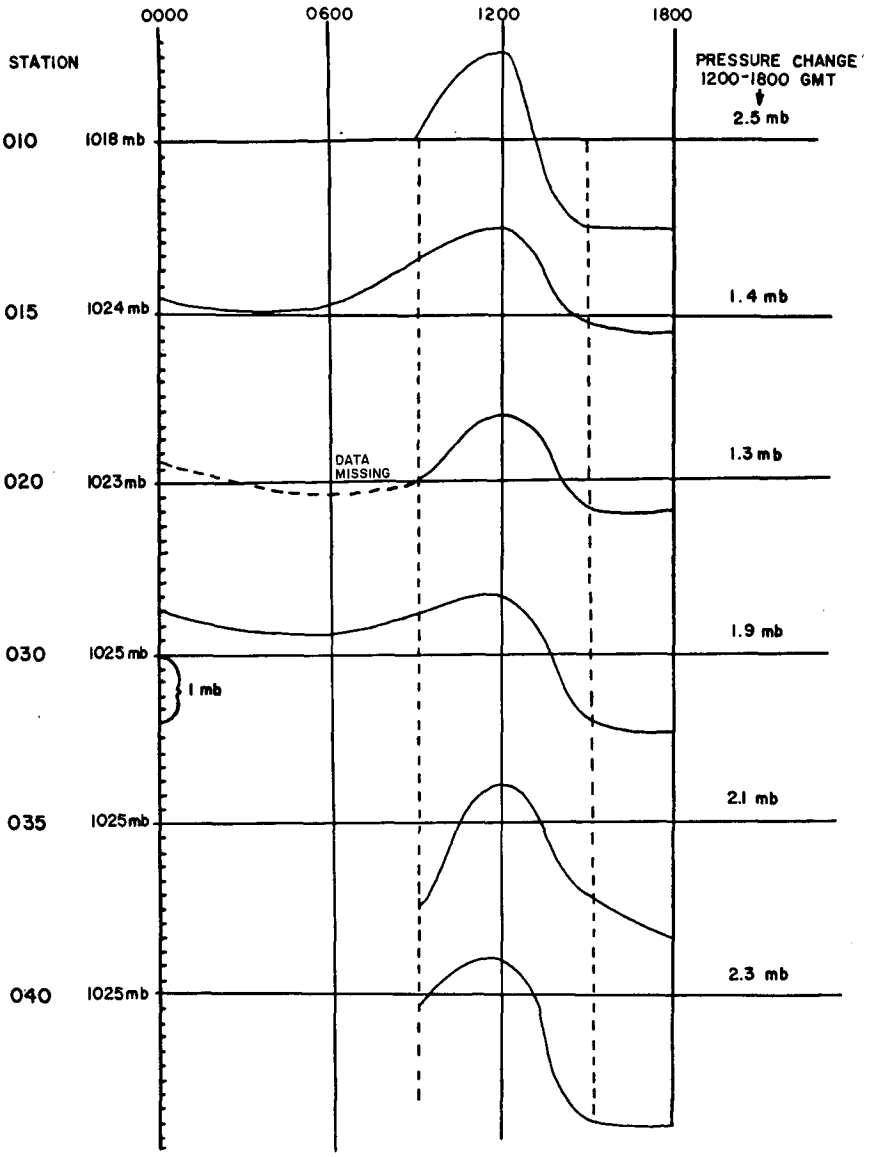

FIG. 5. Semidiurnal pressure variations from 0000–1800 GMT 16 December 1965 for six stations of the Canary Island group.

whereas stations 015, 020 and 030 are located, with respect to U_0, at the stagnation point. Since vortex trail formation occurs on the sides of the islands, the former three stations are in an excellent location to indicate pressure oscillations resulting from vortex shedding. Even though the vortex shedding occurs at an elevation higher than the stations, the shedding may still be producing pressure changes at the stations which are very near sea level.

Fig. 5 is a plot of 6-hr pressure changes over a 24-hr period. The period includes the time at which the photographs were taken. Data were missing for stations 010, 035 and 040 at the approximate time (calculated in later sections) of vortex shedding. Though vortices could be shedding at the time of the photographs, time (and also phase) is not established, and the following discussion is thus merely speculative.

Determining the manner in which the pressure changes occur is made possible by using the net pressure change in the past 3 hr and temperature-pressure groups of synoptic data at the six stations. These plots suggest that the primary pressure change at a given station is due to semidiurnal pressure variations. However, the comparatively larger magnitude of the semidiurnal pressure changes from 1200–1800 GMT at stations 010, 035 and 040, as compared to the semidiurnal pressure changes at stations 015, 020 and 030, suggests that possibly part of the semidiurnal pressure changes at the former three stations was not caused by the semidiurnal wave, but may well be due to vortex shedding.

Assuming the mean pressure change due to semidiurnal effects is 1.0 (Jenkins, 1945), then stations 010, 035 and 040 have differences in magnitudes of changes of 1.5, 1.1 and 1.3 mb, respectively, after the semidiurnal variation is removed. Though the sample size is small in this instance, the pressure difference between the two groups of stations is significant at more than 1% (student t-test).[3] Thus, it is quite probable that the differences in magnitude of changes at stations 010, 035 and 040 were caused by something other than the semidiurnal pressure variation. The values of 1.5, 1.1 and 1.3 mb compare well with the value of 1 mb suggested by Wilkins (1968) for vortex shedding.

All of the above stations were under the influence of the weak pressure gradient typical of a high pressure area, and their pressures have been reduced to sea level. Any error resulting from reducing the pressures to sea level is probably negligible since the stations are very near sea level on the islands. The pressure differences between the two groups of stations are rather large to be accounted for by instrument error. Therefore, the above explanation of aerodynamic effects seems reasonable.

5. Physical considerations

The concept of the diffusion of vorticity can be used to estimate the growth and decay of vortices shed from the islands (Chopra and Hubert, 1965). Since divergence effects (and thus, by implication, vertical motions) in the vorticity diffusion equation are neglected in the region of the vortices considered, speculation concerning the dynamics of cloudiness is desirable.

The layer is presumed to be very shallow and stable. Therefore, it seems possible that the shedded vortices simply disturb the cloudy area in the wake of the island. "Visible" vortices are thus created. Heating from the ocean surface may well enhance the cloudiness in a manner analogous to a process observed by Greenly (1969).

Vortex trails (discernable with dye tracer) were formed in an open-flow channel. Several experiments were performed with and without heating from below the channel. In those cases where there was heating at some distance downstream, some vortices exhibited an apparent rebirth after having broken up over the non-heated area. This was a random vortex enhancement, and might be attributed to a chance encounter and interaction between the toroidal circulation of a convective cell and the vorticity field of a decaying Kármán vortex. In the atmospheric case, the cloudiness in the vortex trail downstream from the island may well be a result of slight vertical convective motions caused by heating from the ocean surface below. At this time, no attempt is made by the author to include the third dimension in the calculations.

[3] This tests the departure of a sample of mean $\bar{X}$ from a hypothetical mean μ by computing the ratio: $(\bar{X}-\mu)\sqrt{N-1}/s$, where N is the sample size, and s the sample standard deviation.

6. Associated equations

The solution to the standard form of the vorticity diffusion equation

$$\zeta=\frac{k}{4\pi\nu t}\exp(-r^2/4\nu t), \tag{1}$$

is used, where the coordinates are relative to the center of a moving vortex. Here ζ is the vertical component of vorticity, k the strength of *line* vortex in an infinite medium, ν the kinematic coefficient of molecular viscosity, r the radial distance from the center of a vortex, and t time. This expression is smaller by a factor of $1/(2\pi)$ than the expression for ζ derived by Chopra and Hubert (1965). This discrepancy is explained in detail by Wilkins (1968).

Following the reasoning of Wilkins, the tangential speed at distance r from the vortex center is given by

$$V_\theta=\frac{1}{2\pi r}\int_0^r \zeta(2\pi r dr)=\frac{k}{2\pi r}[1-\exp(-r^2/4\nu t)]. \tag{2}$$

We now define r_m as the radial distance from the center of the vortex to the maximum tangential wind speed V_m. Differentiating (2) with respect to r, and setting $\partial V_\theta/\partial r=0$, we have

$$r_m^2=5\nu t, \tag{3}$$

from which,

$$V_m=0.72k/(2\pi r_m). \tag{4}$$

A value for ν can be found from its relationship to the Reynolds number $\mathrm{Re}(=U_0D/\nu)$, where D is the effective cross-stream diameter of the island.

Reynolds numbers in the atmosphere would be at least on the order of 10^{10} if the ordinary kinematic viscosity were used; hence, we modify the definition of the Reynolds number by using the coefficient of molecular viscosity.

The next step is to solve for the Reynolds number Re so that a value for the coefficient of eddy viscosity may be found. Lin (1959) introduced a parameter β which experimentally is independent of the size of the obstacle and depends only on the parameters ν, N and U_0. The relationship is

$$\beta=\mathrm{S}/\mathrm{Re}, \tag{5}$$

where S is the Strouhal number $(=ND/U_0)$, and N is the rate of shedding of vortices from one side of the obstacle. The solid curve in Fig. 6 is a graphical relationship of the Strouhal and Reynolds numbers determined from empirical results for oscillating wakes. In laboratory experiments, β ranges from 10^{-3} to 2.5×10^{-3} whenever a vortex street is evident. In their article, Chopra and Hubert (1965) suggest that β will have a wider range for irregular objects such as islands. A value for β of 10^{-3} is assumed for each case in this study in order to achieve consistent results.

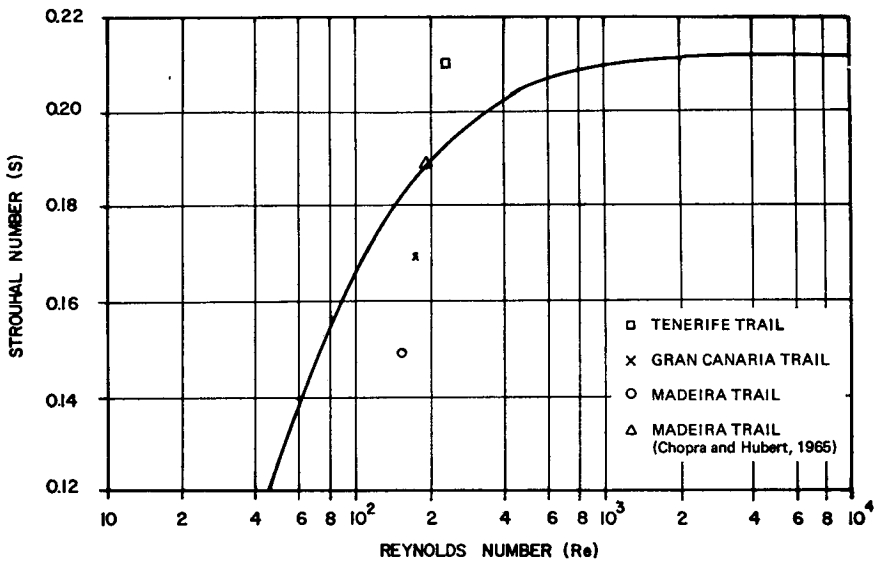

FIG. 6. Experimental curve of Reynolds number vs Strouhal number (Roshko, 1954) with data points for island wake trails.

The rate of shedding N of the eddy pairs is given by

$$N=U_e/a, \tag{6}$$

where U_e is the translation speed of the eddy and a the longitudinal spacing between two eddies of like circulation. The theory, involving the sense of circulation in the formation region of bluff bodies, is treated in detail by Gerrard (1965).

Fig. 7 illustrates the classical Kármán vortex street and relates a, h and L ,the distance parameters between the eddies; L is a distance which can be measured from the photographs, while h and a require a distinct trail of several vortices, and are thus difficult to obtain directly.

By laboratory experiment, the range of the ratio h/a has been observed as $0.28<h/a<0.52$. For this study a value of 0.39 is used for h/a since it is within the laboratory range and also since it makes the equality $\coth(\pi h/a)=\pi h/a$ true. This equality must be satisfied in order that the derivation of the relationship

$$4\pi(h/a)(U_e/U_0)(1-U_e/U_0)=1, \tag{7}$$

by Chopra and Hubert (1964), be valid. From the value

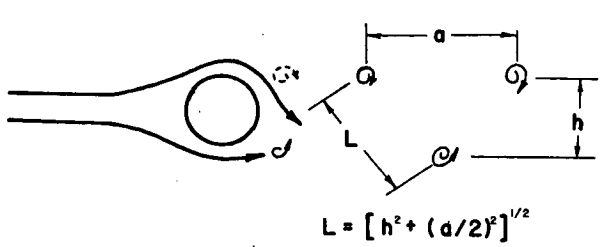

FIG. 7. Schematic illustration of vortex shedding for flow around a cylinder.

$h/a=0.39$, the mean wind flow U_0, estimated synoptically, is 7 m sec^{-1}, and from (7), U_e is calculated as 5 m sec^{-1}. Using U_e, N can be found (6), then S and Re from (5), and finally, $\nu=\beta U_0^2/N$. The quantity r_m^2 can be found knowing ν and t from (3), where $t=d/U_e$, d being the distance from the point of origin to the center of the vortex downstream. This distance can be measured or estimated from the photographs.

As the vortex translates downstream, the center of the vortex moves at a more or less constant speed U_e, the size of the eddy increases, and its energy decreases. Wilkins derived the following expression for the energy decay of an eddy:

$$\epsilon^*=[k^2/8\pi R^2 t][1-\exp(-R^2/2\nu t)]. \tag{8}$$

This expression is divided by mass to convert to the more usual units for kinetic energy dissipation (erg gm^{-1} sec^{-1}). We choose $R=3r_m$ for this study since the tangential velocity at this radius is negligible compared to the maximum tengential velocity. Where $3r_m>L/2$, the latter value is used for R since the circulations of two adjacent vortices will interfere, and presumably cancel, at this distance. Choosing a finite radius R is satisfactory as long as the vortex kinetic energy is negligible at any radius $>R$.

Table 2 lists estimated and calculated parameters used to compute the rate of viscous dissipation, radial distance from the center of a vortex to the maximum tangential wind speed, and the maximum tangential wind speed for the Tenerife trail, Gran Canaria trail, and the pair of eddies from Madeira Island. The values of ϵ^*, r_m and V_m are also listed in Table 2 for these three cases.

7. Tenerife trail

The foregoing results are applied to the second (the first being somewhat obscured by the Island of Gomera), and the third and fourth eddies of the Tenerife vortex trail. The sea-level width of the island is approximately 48 km. Since the shedding occurs somewhat above sea level, we will assume the effective cross-stream diameter D at the level of the shedding to be about 75% of the sea-level width of the island, or 36 km. As measured from the photographs L is $\sim$77 km.

Using these parameters and the other constants shown in Table 2, the age t of the second eddy of the Tenerife trail is 2.4×10^4 sec. Its maximum tangential velocity V_m is 5.5 m sec^{-1}, occurring at a radius r_m of 12 km, and its kinetic energy dissipation ϵ^* is 1.4 erg gm^{-1} sec^{-1}. A small value of r_m is expected, since this second vortex is in its early stages of development compared to the third and fourth vortices. Likewise, it should have a greater maximum tangential velocity and larger kinetic energy dissipation. The third and fourth eddies have values of 4×10^4 sec, 4.0 m sec^{-1}, 16 km, 0.8 erg gm^{-1} sec^{-1} and 5.6×10^4 sec, 3.6 m sec^{-1}, 18 km, 0.6 erg gm^{-1} sec^{-1} for t, V_m, r_m and ϵ^*, respectively. The computed value of the Strouhal number is 0.21 and the Reynolds number is 210. These parameters are noted in Table 2 along with the other constants previously discussed.

TABLE 2. Measured and calculated parameters.

Parameter	Tenerife Island	Gran Canaria Island	Madeira Island
D (km)	36.2	30.0	46.0
U_0 (m sec^{-1})	7	7	7
U_ϵ (m sec^{-1})	5	5	5
L (km)	77.2	83.7	136.8
h/a	0.39	0.39	0.39
β	10^{-3}	10^{-3}	10^{-3}
h (km)	48.2	51.5	84.6
a (km)	122.3	132.0	217.1
N (sec^{-1})	4.1×10^{-5}	3.8×10^{-5}	2.3×10^{-5}
S	0.21	0.17	0.15
Re	210	170	150
ν (cm^2 sec^{-1})	1.2×10^7	1.25×10^7	2.15×10^7
k (cm^2 sec^{-1})	5.8×10^9	6.3×10^9	10.3×10^9

Four eddies from Gran Canaria Island Trail

	Eddy 1†	Eddy 2	Eddy 3	Eddy 4
Vortex age (t, sec)	1.06×10^4	2.42×10^4	3.32×10^4	5.38×10^4
r_m (km)	11	12	14	18
V_m (m sec^{-1})	11.0	5.93	5.02	3.95
ϵ^* (erg gm^{-1} sec^{-1})	9.4	1.5	0.9	0.5

Three trails analyzed by Chopra and Hubert (1964, 1965)

	Madeira	Tenerife	Gran Canaria
Vortex age (t, sec)	1.06×10^4	1.06×10^4	1.06×10^4
r_m (km)	12	11	11
V_m (m sec^{-1})	11.3	9.5	11.0
ϵ^* (erg gm^{-1} sec^{-1})	12.8	9.0	9.4

Tenerife and Madeira trails of this study

	Eddy 2	Eddy 3	Eddy 4	Madeira Trail
Vortex age (t, sec)	2.4×10^4	4.02×10^4	5.63×10^4	12.3×10^4
r_m (km)	12	16	18	36
V_m (m sec^{-1})	5.5	4.3	3.6	3.3
ϵ^* (erg gm^{-1} sec^{-1})	1.4	0.8	0.6	0.23

† Not shown.

8. Madeira Island trail

The pair of vortices in the left-hand portion of the photomosaic were evidently formed around Madeira Island on 15 December 1965. Chopra and Hubert (1965) analyzed a similar pair of Madeira vortices which were in approximately the same location and which were about the same size as the above pair. The same effective cross-stream diameter used in their study is also used in this study, following their reasoning. On first glance at the satellite picture, one might conclude that it creates doubt about the applicability of the theory to the vortex pair. The vortices in the picture appear to be almost abreast, while the easternmost one should be considerably farther upstream for proper orientation. However, the location is quite consistent with the synoptic data and the amount of wind shear possibly existing at the time.

By using the ratio for h/a previously mentioned and by measuring L, a value of approximately 84 km for h is obtained. For a right triangle to be maintained with L as hypotenuse, h must be oriented N–S. The triangle has thus rotated by some 90°. This implies that due to wind shear the easternmost eddy has gained in its position downstream with respect to its mate of opposite circulation.

Wind speed observations to the northeast of Madeira, in combination with the wind at Madeira, suggest that some wind shear is present, since the center of the high pressure area was just west of Madeira Island and wind speeds increased slightly eastward. Analysis of the pressure pattern, assuming negligible friction effects in the environment, indicated that the shearing effect was still effective for some distance from Madeira Island. Thus, the eddies were influenced by this wind shear for most of the time they traversed the distance from Madeira to their present position. These conditions allow the position of the two eddies to be explained in terms consistent with the Kármán vortex theory.

Fortunately, the westernmost tip of Tenerife is due south of Madeira Island, and the easternmost eddy of the pair is due west of Tenerife. Thus, we can find the distance from Madeira Island to the easternmost eddy by simple geometry. This distance d is approximately 563 km. Using this distance and a translation speed $U_e=5$ m sec^{-1}, a value of 12.3×10^4 sec is obtained for the age of the easternmost eddy.

We must consider also the effect of the wind direction changing during the life of the eddies, since this gives some curvature to the path of the vortex pair, causing an increase in the distance traversed by them. The wind direction just above the frictional layer are well approxi-

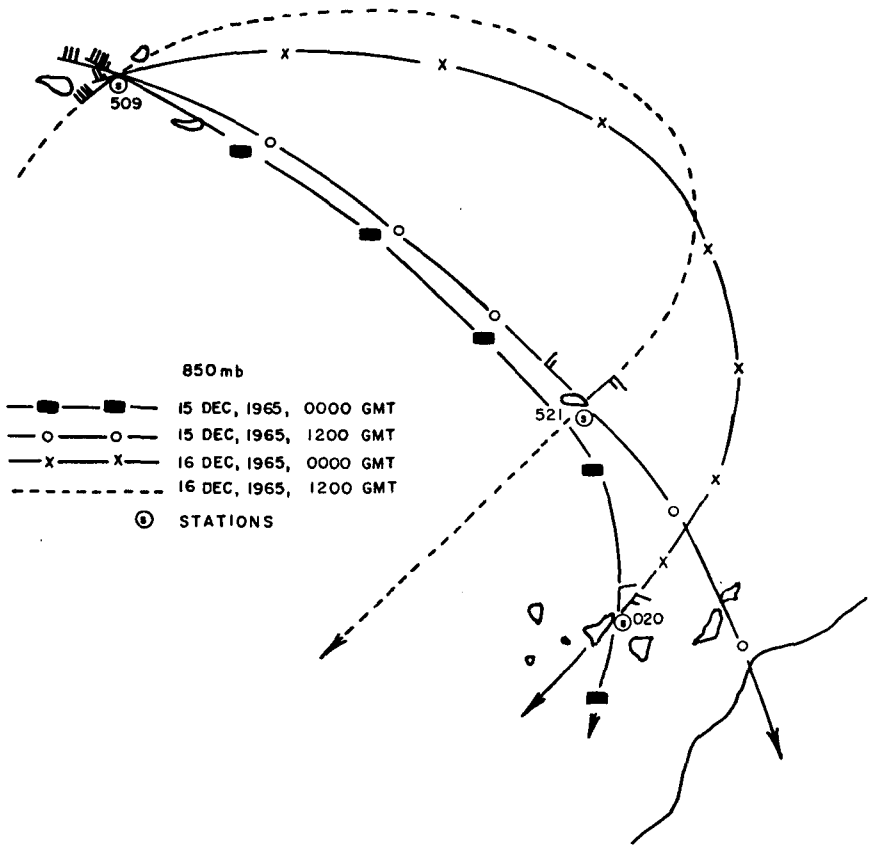

FIG. 8. 850-mb average wind vectors from 0000 GMT 15 December 1965 to 1200 GMT 16 December 1965, showing changing trajectory.

mated by the surface isobar orientation (30°–40°). Synoptic and ship reports on 15 December 1965 indicate northerly circulation; thus, cold air advection is occurring, and above the friction layer, winds will back with increasing altitude. This face is borne out by the 850-mb wind as shown in Fig. 8.

Through the convective cloud layer, therefore, the average wind direction should be a weighted mean of the winds just above the surface friction layer and the 850-mb winds; a good estimate of this case is approximately 350°. It seems likely, therefore, that the vortex pair followed a slightly curved path to arrive at their present position; otherwise, they would have passed directly over the Canary Islands rather than to their west.

With these considerations, a value of 3.26 m sec^{-1} is computed for the maximum tangential velocity with a corresponding radius of 36 km. Since the vortex is some 34 hr old, a larger radius is expected. The kinetic energy dissipation of the eddy is 0.23 erg gm^{-1} sec^{-1}. The Strouhal and Reynolds numbers for the Chopra and Hubert (1965) trail, are 0.19 and 190, respectively. The Strouhal number for the Madeira eddy of this study is 0.15 and the Reynolds number 150, calculated in a manner consistent with the other trails.

9. Gran Canaria trail

Approximate distances of three visible vortices (downstream from Gran Canaria Island) were measured on the photomosaic. The magnitudes of r_m, V_m and ϵ^* were computed for these vortices in the manner previously discussed. A fourth computation is for a vortex (not shown) which was analyzed by Chopra and Hubert (1964, 1965) and Wilkins (1968). Its age is about 3 hr and is included as a hypothetical first eddy in the Gran Canaria trail of this study. The mean wind speed U_0 in the Chopra and Hubert study is the same as in this one. Therefore, the values of 0.39 for the ratio h/a and 10^{-3} for β are applied to their analysis. Also, 75% of the sea-level diameter of the island is again used for the effective cross-stream diameter.

The ages of the second, third and fourth eddies are 2.4×10^4, 3.3×10^4 and 5.4×10^4 sec, respectively. The second vortex has a maximum tangential velocity of 6 m sec^{-1} with a corresponding radius of 12 km. The third and fourth vortices have maximum tangential velocities of 5 and 4 m sec^{-1} occurring at radii of 14 and 18 km. The kinetic energy dissipation rates of the second, third and fourth eddies are 1.5, 0.9 and 0.5 erg gm^{-1} sec^{-1}. These values are listed in Table 2. A Strouhal number of 0.17 is computed and the Reynolds number is 170 for

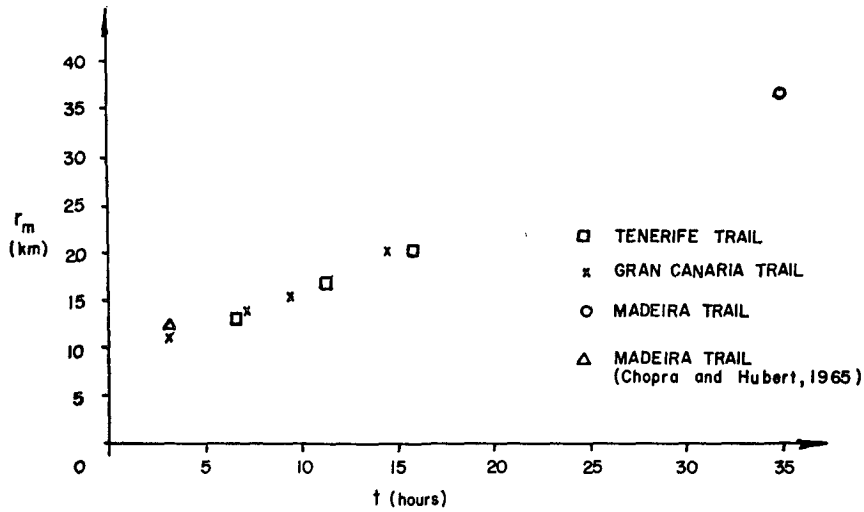

FIG. 9. Variation with time of the radius of maximum tangential velocity for several vortices.

the Gran Canaria trail. These values for the Gran Canaria trail and the Strouhal vs Reynolds numbers for the Tenerife and Madeira vortex trails are plotted on Fig. 6.

Figs. 9, 10 and 11 are the plotted results of r_m, V_m and ϵ^* vs age for the Madeira eddy of this study, the Gran Canaria trail, the Tenerife trail, and the eddy from Madeira Island discussed by Chopra and Hubert (1965). The author computed r_m, V_m and ϵ^* for the latter case, using appropriate parameters given in that study. However, a value of 0.39 is again used for the ratio h/a and a value of 10^{-3} is used for β.

10. Fuerteventura straight cloud street

An average effective eddy viscosity calculated for Tenerife and Gran Canaria Islands is used to calculate Re for the straight cloud street from the 0.8-km peak on Fuerteventura Island. The Reynolds number in the vicinity of this straight cloud street is 35. This compares well with the corresponding value of the Reynolds number in a study by Homann (1936) for a laminar trail which is analogous to the straight cloud street. This gives confidence to the previously calculated values of effective eddy viscosity for the region of the island group, since consistent values are obtained for widely varying obstacle diameters.

11. Conclusions

Results of this study strongly suggest that the von Kármán and related drag theory, along with the theory of vorticity diffusion, may be applied successfully to atmospheric mesoscale eddy patterns. The study en-

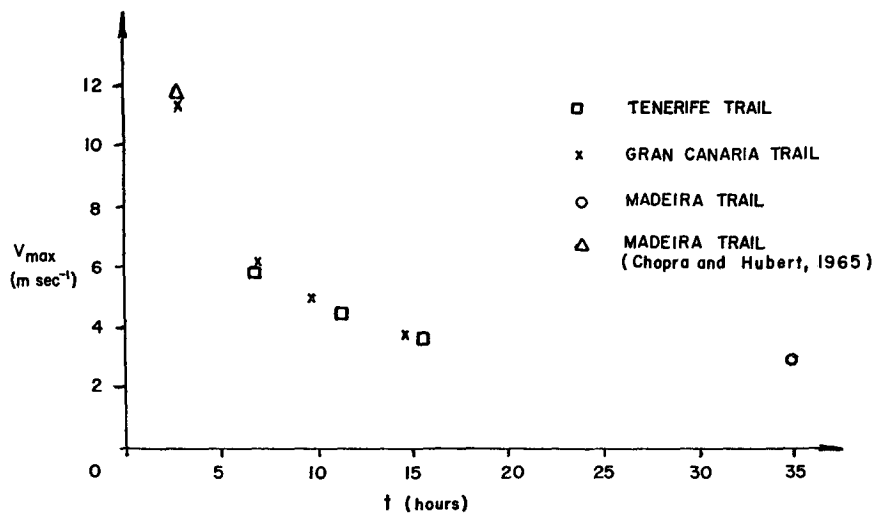

FIG. 10. Variation with time of the maximum tangential velocity for several vortices.

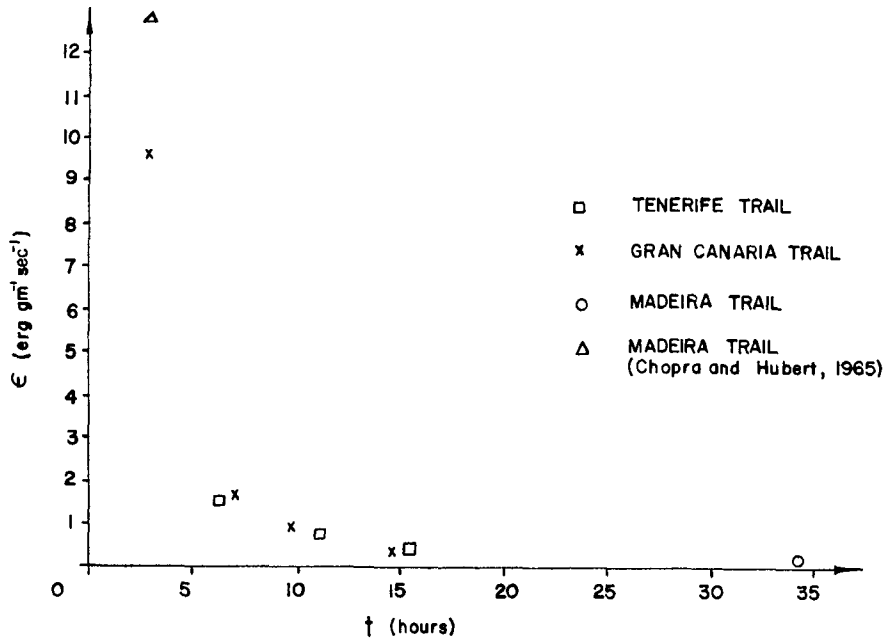

FIG. 11. Variation with time of viscous dissipation of kinetic energy for several vortices.

hances further the idea of using an effective atmospheric eddy viscosity in the dynamical equations in the same sense that molecular viscosity is used in laboratory model experiments to investigate atmospheric vortex phenomena.

Heffter (1965) plotted values of the horizontal coefficient of eddy viscosity as a function of travel period from observations on atmospheric diffusion of various tracer materials. The values of effective eddy viscosity calculated in this study are in close agreement with these plotted values for travel periods up to 20 hr, and for comparable altitudes above ground. The value of effective eddy viscosity for the Madeira eddy is no more than an order of magnitude different from Heffter's values for similar travel periods. However, the values of effective eddy viscosity of this study are still about 2 orders of magnitude greater than the value of 10^5 cm^2 sec^{-1} for the lower atmosphere which is usually accepted for atmospheric convection. More research needs to be done regarding this discrepancy.

The vortex trail situation studied here indicates that there is not any appreciable mutual interference of the trails from the various islands, at least not for the relatively short trails that can be discerned from the photomosaic. This is in agreement with experiments performed in the flow channel on this project. It was found that obstacles separated by at least one obstacle diameter shed separate trails, whereas at closer spacings, or with one obstacle upstream from another a few diameters, the two obstacles will shed a single trail. No configuration was found in which the trails interfere sufficiently to cancel each other, although some individual vortices may not be as well defined as others.

This vortex trail analysis considers all measurable parameters pertaining to vortex streets. The vortices in the photomosaic are in agreement as in the following example. The computed values of the radii of vortex maximum tangential velocities r_m from Table 2 are used as a first approximation to the locations of the maximum tangential velocities around the eddies shown in the photomosaic. Four values of r_m are used to dash in circles for four of the vortices on Fig. 2. This is done for the easternmost eddy of the vortex pair from Madeira Island and the first, second and third vortices of the Gran Canaria vortex trail, since these four vortices are the most clearly discernible in the photomosaic. The first approximation, along with the dashed-in examples, indicates that the maximum tangential winds may be located just inside the region around the vortex where the clouds are in dense bands. Since these bands of clouds around the vortex are narrow and fairly well defined, measurement of r_m from the photomosaic can be reasonably accurate. The measured values of r_m are comparable with the dashed-in examples in Fig. 2 and with the calculated values given in Table 2.

From Fig. 6 it is seen that the Strouhal numbers from this study are within the range of Strouhal numbers observed experimentally. These values are also in excellent agreement with previous atmospheric studies of this kind. It is expected that the Reynolds number for vortex trails will not vary over a range as wide as for oscillating wakes in general. This is because oscillating wakes include vortex trail phenomena as well as oscillating turbulent wakes, which are found up to Reynolds numbers of several thousands.

From Figs. 9, 10 and 11, it is seen that the size of the eddy increases with age, and the maximum tangential wind speed and kinetic energy dissipation of a vortex decrease. Again, this is in agreement with previous studies and hypotheses relating to atmospheric vortex trails.

Practical results of the study are at least three-fold. The first result is that again satellite photographs are used to achieve an accurate analysis of a surface synoptic pattern in a sparse-data region. Secondly, the concept of pressure fluctuations as a result of vortex shedding, suggested by Wilkins (1968), is supported and is related, in a practical sense, to turbulence generated by the island. A third practical consequence follows from the observed and expected persistence times of eddy patterns from both Madeira Island and the Canary Island group. Chopra and Hubert (1964) suggest, if the eddies exist for some period of time, that the meteorological conditions must also have been steady for that period. The available synoptic data reveal no significant meteorological changes during the persistence times of the eddy patterns other than the pressure changes mentioned.

Acknowledgments. The author wishes to thank the Air Force Institute of Technology for providing the scholarship which permitted the study leading to the accomplishment of this manuscript. Also, sincere appreciation is expressed to Dr. Eugene M. Wilkins under whose guidance this research was done. His knowledge and assistance were essential in the completion of this study. Sincere gratitude is expressed to Capt. E. W. Friday for his stimulating discussions and review of the work. Appreciation is also extended to Lt. Col. Lufkin and other members of the Aerospace Sciences Division at the USAF Environmental Technical Applications Center (ETAC), Washington, D. C.

This research was done in connection with graduate study at the University of Oklahoma and supported by the Environmental Science Services Administration under Grants E-41-67(G) and E-188-67(A). The data were furnished by the USAF ETAC. The research would not have been possible without the Gemini photographs supplied by the Manned Spaceflight Center, NASA, Houston, Tex.

REFERENCES

Chopra, K., and L. F. Hubert, 1964: Kármán vortex-streets in the earth's atmosphere. *Nature*, **203**, 1341–1343.

——, and ——, 1965: Mesoscale eddies in wake of islands. *J. Atmos. Sci.*, **22**, 652–657.

Conover, J. H., 1964: The identification and significance of orographically induced clouds observed by TIROS satellites. *J. Appl. Meteor.*, **3**, 226–234.

Friday, E. W., and E. M. Wilkins, 1967: Experimental investigation of atmospheric wake vortex trails. Res. Inst. Rept. ARL-1576-3, University of Oklahoma, 58 pp.

Gerrard, J. H., 1965: The mechanics of the formation region of vortices behind bluff bodies. *J. Fluid Mech.*, **25**, 401–413.

Greenly, G. D. Jr., 1969: An investigation of the formation and maintenance of Kármán vortex patterns. M.S. thesis, University of Oklahoma, 48 pp.

Heffter, G. L., 1965: The mechanics of horizontal diffusion parameters and travel periods of one hour or longer. *J. Appl. Meteor.*, **4**, 153–156.

Homann, F., 1936: Einfluss grosser Zahigkeit bei Stromung um Zylinder *Forsch. Geb. Ingenieurw.*, **7**, 1–10.

Hubert, L. F., and A. F. Krueger, 1962: Satellite pictures of mesoscale eddies. *Mon. Wea. Rev.*, **90**, 457.

Jenkins, G. R., 1945: Diurnal variation of the meteorological elements. *Handbook of Meteorology*, New York, McGraw-Hill., 746–753.

Lin, C. C., 1959: On periodically oscillating wakes in the Oseen approximation. *Studies in Fluid Mechanics Presented to R. von Mises*, New York, Academic Press, 170–176.

Roshko, A., 1954: On the development of turbulent wakes from vortex streets. NACA Rept. 1191, 25 pp.

Wilkins, E. M., 1968: Energy dissipated by atmospheric eddies in the wake of islands. *J. Geophys. Res.*, **73**, 1877–1881.